Ubiquitous UHF Monitoring System for Partial Discharge Detection and Trending

Dr. Jeffrey C. Andle, Jonathan P. Murray,
Maly Chap, and Elkin Baquero
IntelliSAW, Inc.
Andover, MA USA

Jeffrey T. Jordan
Energy Division
Schneider Electric
Smyrna TN USA

***Abstract*—Ubiquitous partial discharge (PD) detection in electrical power assets is needed to provide predictive maintenance for insulators in smart grid critical assets. A low cost solution is discussed that uses simple electronics and algorithms to interpret ultra-high frequency (UHF) signals as a combination of external noise, asymmetric partial discharge (such as corona and other surface discharges), and symmetric partial discharge. The paper describes a device using three UHF frequency bands and a logarithmic detector to provide baseband signal to a digital signal processor (DSP). The DSP employs discrete Fourier transform (DFT) methods to obtain a rapid and succinct quantification of the contribution to the UHF signal from noise sources vs. surface and internal discharge activity. While UHF methods cannot be calibrated in the sense of IEC60270, an apparatus and method for normalizing the response of in situ systems is discussed.**

***Index Terms*-- Corona, discrete Fourier transform, partial discharge, surface discharge, switchgear.**

I. INTRODUCTION

Partial discharge in insulators is one of the leading causes of asset failure in medium voltage (MV) generation, transmission, and distribution assets. One estimate attributes nearly 46% of failures in MV electrical equipment to partial discharge (PD) [1]. Notably a significant number of these PD failures are ultimately humidity driven, and the next highest proportion of failures are thermal in nature. While generators and large power transformers are the bottlenecks of the power grid, the asset with the highest average downtime hours per year are switchgear [2]. Because of the quantity of switchgear installed on the power grid and their downtime, they are the ideal candidate for continuous asset monitoring.

The present work for ultra-high frequency (UHF) partial discharge monitoring repurposes existing receiver electronics from a passive, wireless temperature sensor platform to make PD detection and analysis possible. The temperature monitoring system is based on quartz SAW resonators operating around 433 MHz. The electronics are readily expanded to receive signals as low as 150 MHz and as high as 1500 MHz while using the low cost FR4 board material and compact layout of the original product. While generators, motors and other assets with layered windings tend to emit only high frequency (HF, 3-30 MHz) and very high frequency (VHF; 30-300 MHz) signals, significant activity is observed in the UHF bands (300-3000 MHz) in many important asset classes [3].

The design constraint to avoid frequencies below about 125 MHz was driven by two factors – avoidance of digital noise and conducted radio frequency interference up to 100 MHz along with the FM broadcast band and the receiving antenna physical size relative to the space allowed in a compact medium voltage asset. While this conscious decision was made in the context of UHF detection, the use of high frequency current transformer (HFCT) or coupling capacitors could have provided HF and VHF signal detection while using the existing platform. Since another leading cause of failures in switchgear is flashover [1] resulting from surface contaminants on insulators, the present system consciously avoids capacitive coupling from the energized conductors and insistently uses air gaps to meet the basic insulation level (BIL) safety parameter.

The use of *in situ* measurements inside metal enclosed or metal clad MV switchgear significantly reduces noise contributions from nearby broadcast systems and strongly attenuates the emissions from short range devices (SRD) installed within the neighboring switchgear. The use of a banded UHF PD detection system allows specific frequencies to be filtered out to optimize detection methods and algorithms. UHF PD monitoring has been successfully performed in 40 year old, outdoor, ANSI C37.20 switchgear, within 100 meters of a cellular base station and within multiple high voltage test labs on the latest, and most compact, switchgear designs.

This paper will present the approach to partial discharge detection, including an overview of (a) the UHF band selection, (b) the antenna design constraints, (c) the electronic signal processing chain, and (d) an overview of the digital signal processing scheme. A portable method of synthesizing partial discharge will be introduced, as will the use of this device to "calibrate" an *in situ* system. Finally, preliminary data will be presented.

II. Partial Discharge Detection System

A. UHF Band Selection

The quality of a radio receiver is described by a parameter called the noise figure, which is a dB ratio of the input noise compared to the thermal noise floor. A fundamental challenge of the design is to provide sufficiently low noise figure in the target measurement band while avoiding "jamming" by large signals outside the desired band. Low noise design dictates that the losses should be minimized up to the first low noise amplifier (LNA), which ideally places filtering after the LNA. On the other hand, LNA's are not capable of passing small signals in the presence of a larger, saturating signal. The large signal will saturate the sensitive LNA. Therefore, the band filters were necessarily placed ahead of the LNA.

Size constraints and cost targets led to a decision to employ only three filter bands (300 MHz, 600MHz, and 1200 MHz), which were chosen to minimize interference from the most likely sources of UHF signals. First and foremost inside an MV switchgear is the interference from neighboring systems performing temperature measurements. For this reason the frequencies slightly below and above 433 MHz are intentionally rejected.

Similarly, 868MHz ISM devices in Europe, Asia, and Africa are anticipated, as are 902-928 MHz devices in the Americas. These can comprise high power transmitters in close proximity – for example 1 to 4 W radio frequency identification (RFID) transmitters could be placed within the switchgear. Also in this band are 850 MHz and 900 MHz global system for mobile (GSM) frequencies, and 40 W GSM transmitters could be only meters away.

The lower limits are dictated by the need to reject up to 108 MHz FM broadcast and 100 MHz clock frequencies in the DSP. The upper limits are less clearly defined; however 1800 MHz GSM should also be avoided. The natural losses of the electronics and antenna above 1500 MHz are relied on, as is the shielding of the switchgear. The requirements for rejection at 433 MHz and 860 – 900 MHz determines the crossover frequencies between the three bands. The resulting filter bands are schematically illustrated in Fig. 1.

Low cost, consumer grade inductors and capacitors were used in the circuit, resulting in total losses from the input to the LNA of as much as 6 dB. The LNA noise figure (NF) is 2 dB. The overall noise figure, NF, is 8 dB. The bandwidth, B, in the lower filter is approximately 175×10^6 Hz. The equation for noise floor sensitivity, S, in the absence of an interfering signal is

$$S = -174 + NF + 10\,log_{10}(B). \quad (1)$$

For the lower band the thermal noise floor is -83.6 dBm. A 6 dB improvement in noise floor could be obtained by placing the LNA immediately at the inputs; however antenna switching, function selection, and other required filtering for EMC introduce a significant portion of the losses and the remaining improvements would come at the cost of a severe and debilitating saturation of the input LNA by strong out-of-band radio transmitters. On the other hand, 10 dB of improvement could be obtained by reducing the bandwidth to 17.5 MHz. Similar noise floor results are obtained for "600 MHz" band 2 and "1200 MHz" band 3 as for "300 MHz" band 1.

B. Antenna Design Constraints

A 17cm monopole antenna typically has 3.2 dBi gain and 2 dB of internal losses in the mid UHF (433 MHz). Monopoles are commonly used in handheld surveying tools, given its efficiency; however only large generator circuit breakers are suitably dimensioned to incorporate such a large antenna while maintaining the basic impulse level (BIL) rating of the switchgear. The full height monopole has sufficiently wide bandwidth, but is still incapable of meeting the requirements of the frequency bands identified above.

A number of broadband antenna structures exist [4]. One of the most promising is the Archimedes spiral [5]. Initial measurements were made with a previously-designed [6] Archimedes spiral that was intended to span at least 400 – 950 MHz for colocation of surface acoustic wave (SAW) measurements and RFID measurements. At 300 x 300 x 20 mm, the spiral antenna is suitably dimensioned to most switchgear; although a smaller antenna is ultimately desired. A more significant issue is the bidirectionality of the spiral and the negative reflection from the supporting ground plane. This results in poor antenna efficiency when mounted close to the metal walls of a switchgear. This was notably true at the temperature sensor frequencies around 433 MHz.

A thicker, cavity-backed spiral would be better suited. There exist several recent papers on suitable antennas, and one promising approach is to further miniaturize the spiral antenna [7]. While spiral antennas offer the most uniform properties over a wide range of operating frequencies, they are often too expensive for *in situ* applications. Over time it can be expected that high performance, compact, spiral antennas will become increasingly available at lower costs.

The patch inverted-F antenna (PIFA) was instead selected. The antenna has excellent properties at 433 MHz for the measurement of passive temperature sensors and operates

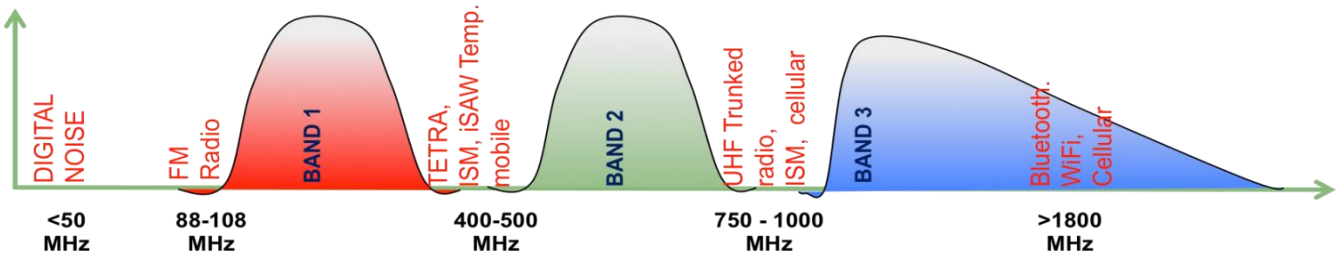

Figure 1 illustrates the three bands selected for the UHF detector and the various known interfering signals to be filtered.

Figure 2 illustrates a typical PIFA S11 where deep resonances represent high efficiency. There is room for improvement at 300 and 600 MHz; however the antenna is seen to operate well in switchgear.

reasonably well over much of the selected UHF bands, as seen in Fig. 2. Whereas the spiral antenna is inherently broadband, the PIFA is multi-band with many broad resonances.

The construction is such that all metal parts are bonded to protective earth at 50-60 Hz and the entire metal structure is encased in 3 mm thick flame resistant (UL94-V0) acrylonitrile butadiene styrene (ABS) plastic to ensure proper safety requirements are met. The dielectric strength is 32 kV/mm, providing a functional insulation to a working voltage of 96 kV. While the ABS should not be solely relied upon to provide safety isolation, it provides supplemental insulation that more than makes up for the 43 mm reduction in air gap with respect to working voltage and BIL ratings. At 200 x 175 x 43 mm, the antenna is well suited to even the most compact switchgear designs.

C. Electronic Signal Processing Chain

The underlying temperature monitoring platform uses quartz SAW resonators as passive, remote temperature sensors. The SAW resonators have a very well defined resonant frequency in the UHF band and a very reproducible frequency-temperature dependence. The sensors are measured by sending a series of UHF pulses, coherently accumulating the back-scatter echoes from the resonant sensors, and computing the resonant frequencies. The resonant frequencies then provide the necessary information on temperature.

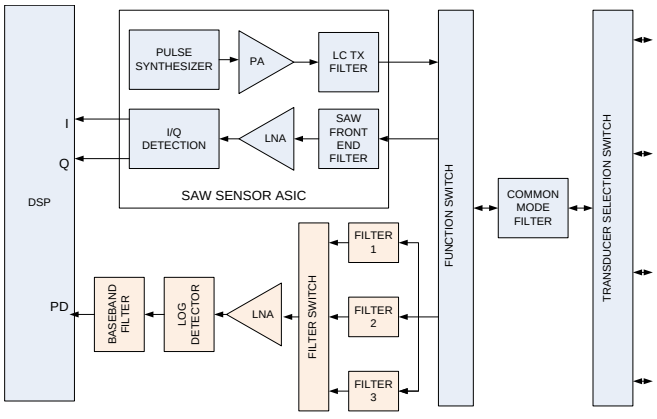

Figure 3 shows existing SAW sensor measurement subsystem (blue) and added electronics for PD monitoring.

Such systems will typically have a digital signal processor (DSP) and analog to digital converters (ADCs) and either discrete radio electronics or an application-specific integrated circuit (ASIC). The present interrogation systems employ a highly integrated and optimized RF ASIC with an external SAW front end filter and receive/transmit (RX/TX) function switch, as shown in Fig. 3. A 100 MHz high-pass, common-mode filter separates the RX/TX function switch from a transducer selection switch for electromagnetic compatibility (EMC) and electromagnetic interference (EMI).

The transducer ports have protective circuitry against electric fast transients and provide additional EMC/EMI protection. The core functionality is a mature and well-established technology [8]-[11].

When adding circuitry for partial discharge detection, care must be taken not to disturb the matching of the transducers to the SAW front-end filter or to undermine the excellent rejection of the SAW front-end filter and internal filters. The SAW sensor's interrogation pulses also must not couple into the PD subsystem's LNA. Since PD is a broadband phenomenon, the transducer interface and common mode filters must provide good impedance match over a wide frequency range. The filter bank must reject switching transients from elsewhere on the PCB and insertion losses must be minimized.

The sensitivity of the PD system will determine the minimum detectable apparent charge. Sensitivity is limited by the insertion loss between the transducers and the PD subsystem's LNA, and the LNA's noise figure, as discussed above. The subsystems required for EMC/EMI compliance with safety and radio emissions (e.g. 4KV impulse level electric fast transient) are not necessarily compatible with low noise figure over very wide bandwidths. While the sensitivity required for reliable PD detection at picocoulomb (pC) levels of apparent charge depends on the transducer and the equipment under test, it can be shown that LNA gain in excess of 20 dB is not especially beneficial. The noise floor is seen to be on the order of -84 dBm while the log detector has a -65 dBm sensitivity.

If a larger number of narrower bandwidth filters were employed, e.g. with 17.5 dB bandwidth, then an LNA gain of 30 dB would be needed to capitalize on the lower noise floor. There are significant challenges in providing gain significantly higher than 40 dB in compact equipment without incurring internal oscillations and there is little benefit unless the bandwidth of the filters were to be significantly reduced.

Following the logarithmic detector, there is a baseband filter that rejects signals with modulation characteristic of SAW interrogation, that is, signals with baseband frequency content below 300 KHz. It also rejects other low frequency modulation as well as signal content above the response frequency of the logarithmic detector of 6 MHz. Finally, it provides a peak detector with an RC time constant decay.

This last step is a critical differentiator between higher-cost, analytical instruments and the present, ubiquitous, early warning detector. Analytical instruments performing phase resolved partial discharge (PRPD) require nanosecond-scale

digitization of fast transients to count and quantify events associated with PD. They must then display large data sets that convey significant amounts of complex information. These analytical instruments often require a trained scientist to interpret the data set. In contrast, the present algorithm allows the use of low cost, microsecond-scale digitization with "on the fly" conversion to concise information. Although analytical detail is lost, the results are readily presented to the "big data" tools pervasive to the smart grid, enabling system-wide trending of developing asset failures using low-cost, autonomous instrumentation.

D. Digital Signal Processing Scheme

The DSP is programmed to perform analog to digital (ADC) conversions with a sampling time just slightly longer than the computation time required to progress the digital filters. For each sample, nine discrete Fourier transform (DFT) calculations are updated. The process is iterated over an even number of power frequency wave periods.

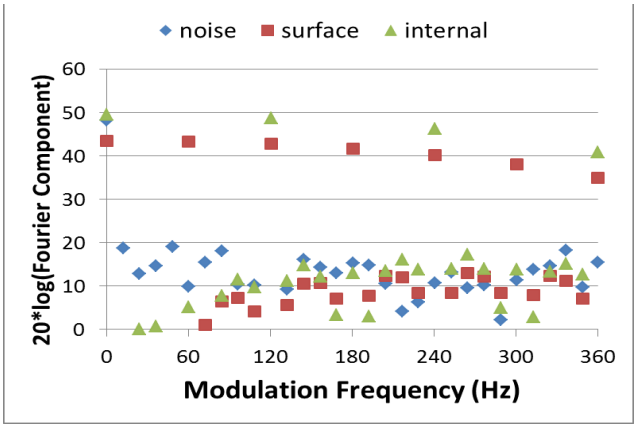

Figure 4 illustrates the DFT content for a 60 Hz line frequency when presented with noise, surface, and internal discharge signals.

Noise is always present – either at constant amplitude or with modulation uncorrelated to the line frequency. Absent any significant external, modulated source, noise will manifest itself as a constant term (zero frequency modulation of the logarithm of the UHF received power) plus low levels of modulation signal in all of the DFT terms at nonzero frequency, shown as diamonds in Fig. 4.

Corona discharge occurs primarily on the negative half cycle of the power waveform [12], where electrons emitted from the metal ionize the air. Corona (also called surface discharge or asymmetric discharge) presents significant DFT results at both odd and even harmonics of the power line frequency, shown as squares in Fig. 4.

Discharge within the bulk of materials occur approximately equally for positive and negative polarity portions of the power cycle. Because of this, internal or symmetric partial discharge presents as even harmonics, shown as triangles in Fig. 4.

At the onset of PD, where discharges occur in a narrow time window near the peak voltage, the DFT responses, and therefore the instrument response, are linear in the number of events. The system measures a cumulative PD activity per power cycle. On the other hand, the DFT terms are logarithmic in the magnitude of individual PD events. By counting the number of events, it is possible to estimate the geometric mean of the PD activity as

$$\overline{p} \approx \frac{\sum_{i=1}^{N} log(p_i)}{N}, \tag{2}$$

where $\overline{p}$ is the mean discharge event magnitude, N is the number of discharge events per measurement period, and the sum of pi is determined from the DFT terms as

$$\sum_{i=1}^{N} log(p_i) = A \begin{pmatrix} \sqrt{x^2 + y^2 + z^2} \\ -B\sqrt{u^2 + v^2 + w^2} \\ -C\sqrt{r^2 + s^2 + t^2} \\ -D \end{pmatrix}. \tag{3}$$

A, B, C, and D are calibration coefficients where B and C are typically 1 and D is typically 0. The terms r, s, and t are DFT results at frequencies selected to indicate noise level, u, v, and w are selected to represent corona, and x, y, and z are selected to represent symmetric discharge processes.

As the PD activity fills an increasing large portion of the power waveform, the integral of the DFT is no longer the linear summation of (2). Instead the integral is decreased by a trigonometric factor. This quantitative desensitization at increasing PD activity levels represents a saturation effect and has no impact on early warning.

III. Portable Discharge Synthesizer

The portable discharge synthesizer is a simple, yet effective tool that uses 5V power from a laptop's USB port to power a circuit. A microprocessor generates trigger pulses to a flyback transformer, allowing a 4 µs charge time and a 40 µs repetition rate. Bursts of 1 – 50 pulses may be created at the positive peak, negative peak, or both. Each pulse generates a nominal 1000 V ramp in tens of nanoseconds onto a 1 pF gas discharge tube (GDT). The result is a 1 nC discharge within the GDT with nanosecond-scale collapse of the stored charge.

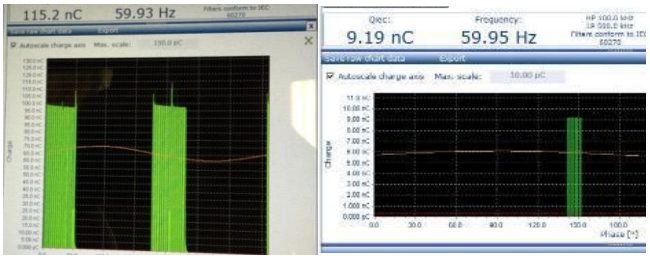

Figure 5 illustrates the response of a PD Smart in direct measurement mode for a PD synthesizer having no resistor (left) and 20KΩ (right).

A parasitic ringing of the flyback transformer is also seen, which appears to also comprise PD to an IEC 60270 system, such as a PD Smart analyzer. Depending on the resistive isolation of the GDT from the flyback transformer, this ringing can appear to as much as 100 nC down to trivially small levels. Fig. 5 illustrates two tests with resistive values of 0 Ω and 20 kΩ, with 115 nC and 9.19 nC apparent discharges, respectively. Higher resistor values are expected to provide IEC60270 measurements approaching the estimated

1 nC per pulse. While this is a large level of PD, it is still suitable for full-scale validation of an in situ system.

The PD synthesizer is distinct from other "UHF calibration" systems that use a square wave pulse and internal circuit board traces to transmit broadband signals. The present device generates physical discharges in a well-defined structure at well-defined voltages and capacitances. In addition to quantitative analysis using the PD Smart system, a PDS 100 UHF surveyor was also used to validate the synthesizer. Significant UHF emissions were observed over the instrument's operating range.

In principle the synthesizer can be used to normalize the coefficient, A, of (3) by placing the synthesizer in a location central to a region in which PD activity is likely and then observing the system response. In practice this will normalize one installation to be similar to another; however it will not accurately calibrate a system. Different discharge processes have differing UHF emission efficiency, so it is not truly a calibration process. On the other hand, IEC 60270 is only able to calibrate the signal path from the contact point through the instrumentation chain, and information on the actual defect process is still elusive 0.

IV. Preliminary Data

A. *Synthesized PD in a Grounding Potential Transformer*

A 22 kV grounding potential transformer (GPT) was instrumented with a partial discharge measuring system. The installation was made under live conditions using a dielectric tool to slide the magnetically mounted antennas along the steel walls into place. The antenna locations are shown in Fig. 6.

Figure 6 shows the front safety barrier of the GDT with PD antennas on the left and right walls.

A PD synthesizer was used to demonstrate system functionality. The synthesizer was located at the lower left gap between the side wall and the safety barrier and generated either 20 pulses of PD (10 positive and 10 negative) or 20 pulses of surface discharge (negative only). The response was measured using an IntelliSAW CAM-4 system and a screen capture is shown in Fig. 7. The estimated cumulative discharges were 20 nC, suggesting A ≈ 10 pC in (3).

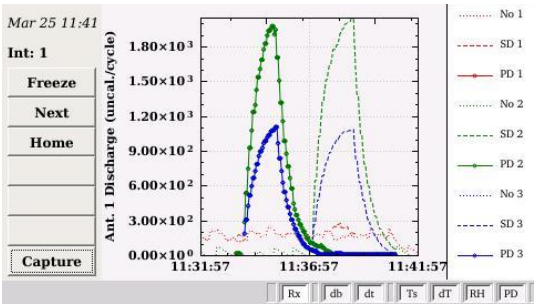

Figure 7 shows a screen capture of the 600 and 1200 MHz responses to synthesized PD and Corona discharges in a 22 KV GPT.

B. *Testing at Switchgear Manufacturers*

One test was performed in a 17.5 KV, 1250 A switchgear with 31.5 kA fault current rating in a 650 mm cabinet. Measurements of the de-energized system showed no ambient interference. When energized to 10 kV only very small signals were obtained. The isolation distance of the energized phase to ground was artificially reduced, resulting in increasing levels of PD as the voltage was raised and lowered. Finally, 15 kV was applied with spacings of nominal value, 5, 4, and 3 cm; the results of this last test are presented in Fig. 8. The levels at 15kV and 3cm spacing are comparable to the response for 40 nC cumulative of synthesized PD in other tests. However, since the synthesizer was not tested in the switchgear, a direct comparison is not possible. Nonetheless, the results of Fig. 8 suggest discharges on the order of 20 nC cumulative at 4 cm and as high as 50 nC cumulative at 3 cm.

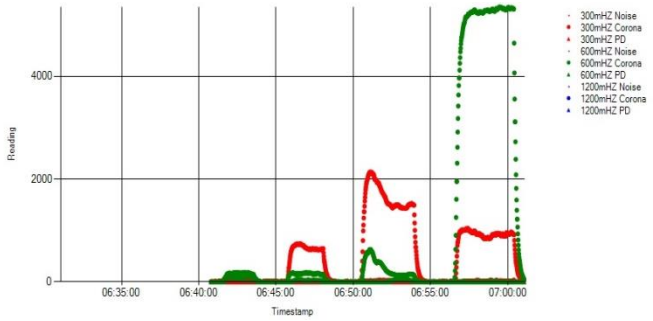

Figure 8 illustrates the response to 15kV applied through normal insulation distances and then reduced to sub-standard spacing.

A second test was performed in a 15kV switchgear. This test was performed without side panels and with incomplete shielding of external UHF sources. Noise was identified in the "600 MHz" band, while both "300 MHz" and "1200 MHz" bands indicated small levels of corona activity at full rated voltage as illustrated in Fig. 9. Based on the synthesizer results of Fig. 7, there may be on the order of 400 – 600 pC cumulative at the peak response (14:00 timestamp) and down to 50-200 pC (the noise floor) otherwise.

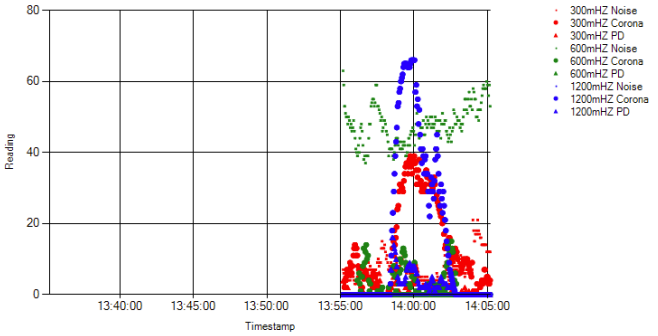

Figure 9 illustrates the response to voltage stress applied through normal insulation distances.

Whereas the first test sought to cause various levels of PD by intentionally violating spacing rules at the operating voltage, the second factory test sought to validate that the system, as designed, had suitably low levels of intrinsic partial discharge under stress.

The logarithmic response of the system allows measurement of hundreds of discharges per power cycle at tens of nC levels, as produced by the synthesizer or failing switchgear. It also suitably detects a range of naturally occurring PD induced at various levels, down to the "noise floor" of new, compliant switchgear.

C. On-Line Testing in Outdoor Switchgear

An outdoor substation consisting of two 110 kV/13.8 kV transformers two outdoor switchgear having drawout breakers and a connecting bus duct, was instrumented with continuous PD monitoring equipment. One switchgear faces a cellular tower at a distance of 50 meters, and, even with the shielding of the cable compartment doors, the noise in the 600 MHz band is too large. These systems still operate properly in the 300 and 1200 MHz bands without interference

The second switchgear, with data presented in Fig. 10, is 60 meters away from the tower but with the cable doors oriented away from it. This system shows virtually no noise in the 600 MHz band. A bus tie switch at the far end from the transformer was the only system instrumented in this switchgear. The large and persistent 300 MHz signal corresponding to corona discharge is potentially conducted from the transformer or an adjacent, un-instrumented switchgear. More interesting are the 1200 MHz partial discharge and corona spikes that correlate to saturating relative humidity (light blue) in the attached bus duct.

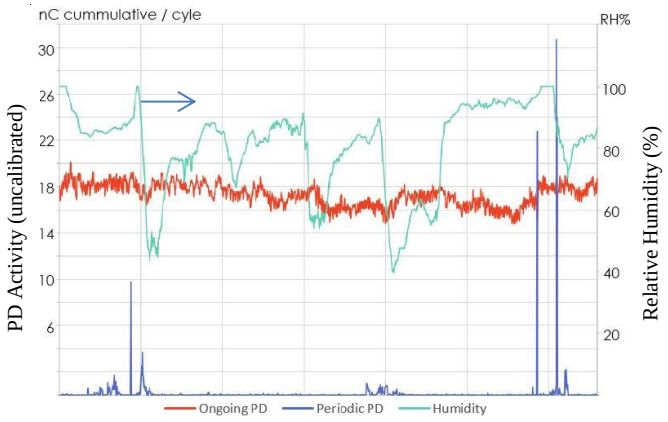

Figure 10 illustrates long-term corona activity in the 300 MHz band and abrupt PD and corona activity in the 1200 MHz band. Abrupt activity correlates to saturating humidity.

V. CONCLUSIONS AND FUTURE WORK

The present work demonstrates that a PD detection system using band-pass filtered UHF detection is capable of avoiding strong interfering signals at close proximity. Analysis methods that employ simple, but elegant, discrete Fourier transform methods can provide the clear and concise reporting of PD events needed for long-term trending. In addition, the system now combines passive, non-contact sensing of temperature and partial discharge with humidity and ambient sensing to make available a comprehensive solution for real-time continuous critical asset monitoring. The combined system addresses most of the electrical failure mechanisms of switchgear and other critical power assets.

Future hardware developments will focus on three areas, improved antenna performance, improved noise floor, and improved linearity of the response. In particular, the antenna impedance match at 600MHz could be improved. The estimation of the number of defects, N, is not fully implemented and the calibration coefficient is linear in N and logarithmic in p_i.

The first two improvements speak to improving sensitivity while the latter speaks to a transition from an "indicator" to an analytical measurement system. A fourth, and more important, improvement relates to improved analytical software to simplify and automate the trending of PD data over a distributed power grid. The true strength of ubiquitous monitoring is the power of "big data" to predict and schedule maintenance needs system-wide.

ACKNOWLEDGMENT

The authors wish to thank Falk Werner and Ken Elkinson for assisting with lab data using Doble PD Smart and PDS 100 systems. They would also like to thank Tony McGrail for insightful discussions.

REFERENCES

[1] Gabe Paoletti and Martin Baier, "Failure contributors of MV electrical equipment and condition assessment program development", Industry Applications, IEEE Trans. on (Volume:38, Issue: 6), Nov/Dec. 2002, pp. 1668-1676..

[2] Claude Kane and Alexander Golubev, "How advanced on-line partial discharge diagnostics can make you a hero", Available: http://www.dynamicratings.com/US/Application/Switchgear%20and%20Cables/Technical%20Papers/TP10.pdf.

[3] Ricardo Albarracín Sánchez, Medida de descargas parciales en radiofrecuencia, PhD Dissertation, Universidad Carlos III de Madrid, February 2014.

[4] M. Vahdana, " Low-profile, ultra wideband and dual polarized antennas and feeding systems", Ph.D. dissertation, l'Ecole Nationale Supérieure des Télécommunications, 2008

[6] J. L. Volakis, M. W. Nurnberger, and D. S. Filipovic, "A broadband cavity-backed slot spiral antenna", in IEEE Antennas and Propagation Magazine. Vol. 43, NO. 6., pp. 15-26. Dec. 2001

[7] J. C. Andle and C. J. Lanzl, "Use of a wireless temperature monitoring system as an early warning detector of partial discharge", unpublished, submitted to IEEE ISGT, Malaysia 2014.

[8] H-B Kim, K-C Hwang, and H-S Kim, "Cavity-backed Two-arm Spiral Antenna with a Ring-shaped Absorber for Partial Discharge Diagnosis", in J. Electr Eng Tech. Vol. 8, No. 4: pp. 856-862, 2013

[9] V. Kalinin, "Modelling of a wireless SAW system for multiple parameter measurement", in Proc. of 2001 IEEE Int'l Ultrasonics Symp., pp. 1790-1793, October 8-10, Atlanta, USA, 2001.

[9] J. C. Andle, S. Sabah, D. S. Stevens, S. J. Jumani, M. Baier, B. W.A. Wall, T. Martens, and R. Gruenwald, "Temperature Monitoring System Using Passive Wireless Sensors for Switchgear and Power Grid Asset Management", unpublished, presented at MNC-CIGRE/CIRED MALAYSIA, T & D Asset Management Workshop, 8-9 December 2010.

[10] D. S. Stevens, J. C. Andle, S. Sabah, S. J. Jumani, B. W.A. Wall, M. Baier, T. Martens, and R. Gruenwald, "Applications of Wireless Temperature Measurement Using SAW Resonators" in Fourth In'l Symp. on Acoustic Wave Devices for Future Mobile Comm. Systems, 2010, pp. 61-68, Chiba University, Japan.

[11] J. C. Andle and C. L. Lanzl, "On-Line Wireless Passive Temperature Monitoring For Smart Grid Predictive Maintenance", in SmartElec 2013, pp. SASP22-31, Vadodara, India.

[12] P. J. Moore, I. Portugués, and I. A. Glover, "A Non-Intrusive Partial Discharge Measurement System based on RF Technology", Power Engineering Society General Meeting, 2003, IEEE (Volume: 2).